Transport regimes for exciton polaritons in disordered microcavities

A. N. Osipov [1], I. V. Iorsh,[1,2] A. V. Yulin [1], and I. A. Shelykh[3,1,2]

[1]*Department of Physics, ITMO University, Saint Petersburg 197101, Russia*
[2]*Abrikosov Center for Theoretical Physics, MIPT, Dolgoprudnyi, Moscow Region 141701, Russia*
[3]*Science Institute, University of Iceland, Dunhagi 3, IS-107 Reykjavik, Iceland*

Light-matter coupling in a planar optical cavity substantially modifies the transport regimes in the system in the presence of a short-range excitonic disorder. Based on a master equation for a resonantly coupled exciton-photon system, and treating disorder scattering in the Born-Markov approximation, we demonstrate the onset of ballistic and diffusive transport regimes in the limits of weak and strong disorder, respectively. We show that transport parameters governing the crossover between these two regimes strongly depend on the parameters characterizing light-matter coupling, in particular Rabi energy and detuning between excitonic and photonic modes. The presented theory agrees with recent experimental data on transport in disordered organic microcavities.

I. INTRODUCTION

Bright excitons are bound states of electrons and holes, which can be created optically in direct band gap materials. These composite quasiparticles can be used for a variety of optoelectronic applications [1–3]. There exist, however, certain obstacles, which make direct applications of excitons problematic. In particular, being massive particles optically created, excitons usually have small group velocity. In realistic samples, where disorder is always present, this leads to very short dephasing times and, consequently, short characteristic propagation lengths of excitons, which becomes a major problem in such fields as photovoltaics [4,5].

Excitonic transport and the ways to enhance it were widely studied in the literature [6–11]. An attractive option consists of resonant coupling of an excitonic transition to a photonic mode of an optical cavity. If the energy of this coupling exceeds all characteristic broadenings in the system, the regime of strong light-matter coupling is established and a novel type of quasiparticle, the exciton-polariton, is formed. Being of hybrid nature, polaritons combine the properties of light and matter particles forming them. In particular, from the photonic component they inherit extremely small effective mass (about 10^{-5} of the mass of free electrons) and macroscopically large coherence length [12], while the presence of the excitonic component enables the sensitivity of polaritons to external potentials and, in particular, allows efficient polariton scattering on excitonic disorder potential [13].

Recently, it has been observed that mixing with the photonic mode significantly modifies the transport properties of polaritons at low temperatures as compared to bare excitons in both organic [14–19] and inorganic [20,21] microcavities. In general, in samples with high photonic fractions the ballistic transport regime is usually established, whereas crossover to the regime of diffusive transport occurs when the excitonic

fraction is increased, as was recently unambiguously demonstrated in Ref. [14].

This effect has a clear qualitative explanation. Indeed, at low temperatures when short-range impurity scattering gives a major contribution to the transport, it affects only the excitonic part of the wave function of a polariton, while the photonic part remains coherent. This results in experimentally observable narrowing of a polariton's linewidth due to the suppression of excitonic inhomogeneous broadening [20], the effect known as polariton motional narrowing. While the first theoretical description of this effect was developed decades ago [22], a microscopic theory of the crossover between different transport regimes in real space related to it is still lacking. The creation of such a theory is an actual task, specifically in light of the recent revival of experimental activity in this field [14,20].

In the present work we aim to fill this gap. We use the density matrix formalism [23–26] to derive a master equation for polaritons in microcavities in the presence of randomly located impurities. We show that for excitons, equations describing both diffusive [8,27] and ballistic propagation [28] can be derived from the master equation in the limits of strong and weak disorder, respectively. For polaritons, we use the adiabatic elimination technique [29] to get rid of the upper polariton branch in the limit when characteristic energy of the disorder potential is smaller then the Rabi splitting. The analysis of the dynamics of lower polaritons allowed us to demonstrate that the increase of the photonic fraction enhances group velocity of the excitations and suppresses the scattering on a short-range disorder potential, which leads to a crossover from the diffusive to ballistic propagation regime. Expressions for relevant quantitative characteristics describing such a crossover, such as the polaritonic relaxation time and diffusion coefficient [30,31], are derived. Our results contribute to the understanding of the relation between

motional narrowing and regimes of the polariton dynamics in real space.

II. THE MODEL

We consider a 2D planar microcavity formed by two Bragg mirrors with a quantum well (QW) with an excitonic transition embedded in an antinode of a confined cavity mode and brought close to the resonance with it, as shown schematically in Fig. 1. We neglect the effects of polariton nonlinearities in the present study; a finite lifetime is not expected to modify the transport regimes and is neglected in our further discussion. Moreover, the lifetime of photons in high-quality samples can be as long as hundreds of picoseconds [32].

The resonant interaction between excitons and photons leads to the establishment of the strong-coupling regime and formation of cavity polaritons, which will be the focus of our attention. Initially coherent polariton wave packets with controllable parameters can be created in the system by a focused pulse of a coherent light. The presence of a short-range disorder in the QW will create an effective random scattering potential affecting the excitonic part of the polariton wave function, and polaritons will thus gradually lose their coherence. This will affect their real-space dynamics, which will change from ballistic to diffusive, as we will show below.

In the linear regime, when exciton-exciton interactions can be neglected, the dynamics of the system can be described with the following model Hamiltonian:

$$H = \sum_{k}[\varepsilon_x(\boldsymbol{k})b_{\boldsymbol{k}}^{\dagger}b_{\boldsymbol{k}} + \varepsilon_c(\boldsymbol{k})a_{\boldsymbol{k}}^{\dagger}a_{\boldsymbol{k}} + \hbar\Omega_R(b_{\boldsymbol{k}}^{\dagger}a_{\boldsymbol{k}} + a_{\boldsymbol{k}}^{\dagger}b_{\boldsymbol{k}})]$$
$$+ \sum_{\boldsymbol{k}\boldsymbol{k}'} V_{\boldsymbol{k}\boldsymbol{k}'}b_{\boldsymbol{k}'}^{\dagger}b_{\boldsymbol{k}}, \tag{1}$$

where b_k, a_k are excitonic and photonic field operators, $\varepsilon_x(\boldsymbol{k})$, $\varepsilon_c(\boldsymbol{k})$ are the dispersions of bare excitons and photons, Ω_R is the Rabi frequency controlling the strength of exciton-photon interaction, and finally, $V_{kk'}$ is the matrix element of a short-range excitonic disorder potential. In our further consideration we approximate the photonic dispersion by a parabola, $\varepsilon_c(k) = \hbar^2 k^2/2m_{ph}$, where m_{ph} is an effective mass of a cavity photon, and take the excitonic dispersion flat, $\varepsilon_x(\boldsymbol{k}) = \delta = $ constant. The distance

$$\delta = \varepsilon_c(0) - \varepsilon_x(0) \tag{2}$$

is an important parameter of the system governing the percentage of excitonic and photonic fractions in a polariton.

For our purposes it is convenient to represent the Hamiltonian as a sum of the unperturbed Hamiltonian H_0 describing excitons and photons in a spatially uniform system and the perturbation H_V accounting for the interaction of excitons with the disorder,
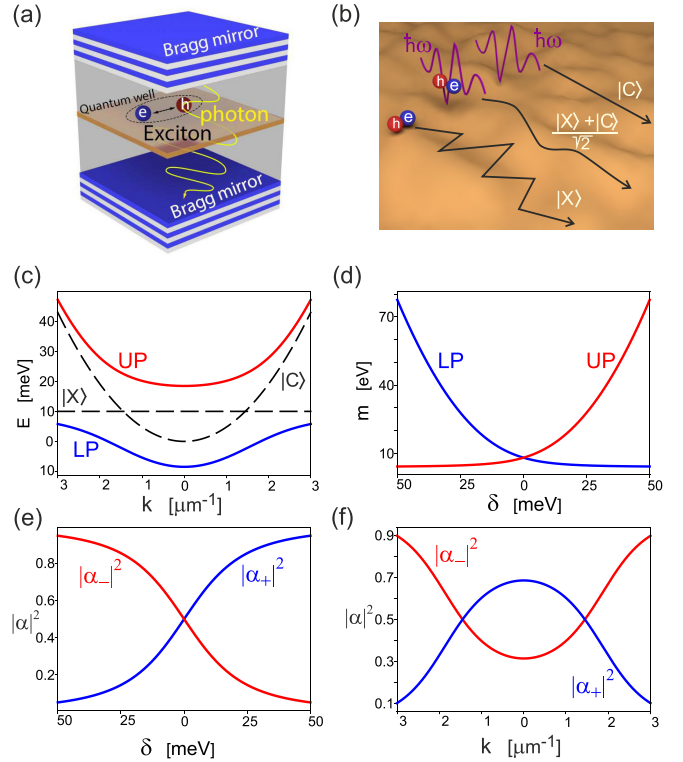
$$H = H_0 + H_V, \tag{3}$$

FIG. 1. (a) Schematic illustration of a microcavity consisting of two Bragg mirrors and a quantum well with an excitonic transition brought close to the resonance with a confined photonic mode. (b) The illustration of propagation of different types of the excitations in the system in the presence of a random short-range potential. Bare excitons have small group velocity, experience strong scattering on the disordered potential and, therefore, are subject to random walks leading to the onset of the diffusive transport regime. On the contrary, photons have very high group velocities, do not experience any scattering on short-range potential at all, and propagate ballistically. Polaritons are hybrid particles for which an intermediate transport regime is established, which becomes closer to ballistic or diffusive depending on excitonic and photonic fractions which can be controlled by change of a cavity detuning. (d) Dispersion characteristics of upper (red solid line) and lower (blue solid line) polaritons calculated for the following parameters of the system: photonic effective mass $m_{ph} = 0.8 \times 10^{-5}m_e$, Rabi energy $\hbar\Omega_R = 12.5$ meV, cavity detuning $\delta = -10$ meV. The dashed black lines show the dispersion of the noninteracting photons and excitons. The hybridization is strongest at the wave vectors corresponding to the crossing of the photonic and excitonic dispersions. Changing the detuning between the resonant frequency of the cavity and the exciton frequency ΔE, it is possible to control both the effective mass of the polaritons [panel (e)] and excitonic and photonic fractions [Hopfield coefficients; panel (g)]. Note that for a given value of the detuning, Hopfield coefficients depend on in-plane momentum of a polariton k [panel (f)].

where

$$H_0 = \sum_{k}(\varepsilon_x(\boldsymbol{k})b_{\boldsymbol{k}}^{\dagger}b_{\boldsymbol{k}} + \varepsilon_c(\boldsymbol{k})a_{\boldsymbol{k}}^{\dagger}a_{\boldsymbol{k}} + \hbar\Omega_R(b_{\boldsymbol{k}}^{\dagger}a_{\boldsymbol{k}} + a_{\boldsymbol{k}}^{\dagger}b_{\boldsymbol{k}})) \tag{4}$$

and

$$H_V = \sum_{kk'} V_{kk'} b_{k'}^\dagger b_k. \tag{5}$$

The first part of the Hamiltonian H_0 can be diagonalized by moving to the polaritonic basis with use of the unitary transformation

$$c_{k+} = \alpha_+ b_k + \alpha_- a_k, \tag{6a}$$

$$c_{k-} = \alpha_+ a_k - \alpha_- b_k, \tag{6b}$$

where $c_{k\pm}$ are operators of upper and lower polaritons, and $\alpha_\pm$ are Hopfield coefficients corresponding to excitonic and photonic fractions in them.

As a result one gets

$$H_0 = \sum_k (E_+ c_{k+}^\dagger c_{k+} + E_- c_{k-}^\dagger c_{k-}), \tag{7}$$

where

$$E_\pm(\boldsymbol{k}) = \frac{\varepsilon_c(\boldsymbol{k}) - \varepsilon_x(\boldsymbol{k})}{2} \pm \sqrt{\left(\frac{\varepsilon_c(\boldsymbol{k}) - \varepsilon_x(\boldsymbol{k})}{2}\right)^2 + (\hbar\Omega_R)^2} \tag{8}$$

are dispersions of the polariton modes. $E_\pm$, $\alpha_\pm$ are illustrated by panels (c)–(f) of Fig. 1.

To describe the dynamics in our system, we start from the Liouville–von Neumann equation for the full density matrix,

$$\partial_t \rho = -\frac{i}{\hbar}[H_0, \rho(t)] - \frac{i}{\hbar}[H_V, \rho(t)], \tag{9}$$

which we treat in the Born-Markov approximation [23,24]. This allows us to get the following master equation:

$$\partial_t \rho = -\frac{i}{\hbar}[H_0, \rho(t)] \\ - \left\langle M_0 \frac{1}{\hbar^2} \left[H_V^I(t), \int_0^t dt' [H_V^I(t'), \rho^I(t)] \right] M_0^\dagger \right\rangle_c, \tag{10}$$

where

$$M_0 = \exp\left(-\frac{i}{\hbar}H_0 t\right) \tag{11}$$

and

$$H^I(t) = M_0^\dagger H_V^I(t) M_0 \tag{12}$$

denotes the scattering Hamiltonian in the interaction picture. The brackets $\langle \ \rangle_c$ denote averaging on the noncorrelated impurity's position (for details see Appendix A).

Spatiotemporal dynamics of a polariton ensemble is determined by a time evolution of a single-particle polariton density matrix [23]

$$\rho_{\zeta_1,\zeta_2}(\boldsymbol{r}, \boldsymbol{r}', t) = \frac{(2\pi)^2}{A} \int \rho_{\zeta_1,\zeta_2}(\boldsymbol{k}, \boldsymbol{k}', t) e^{i(k'r' - kr)}, \tag{13}$$

where $\zeta_{1,2} = \pm$ corresponds to the upper and lower polariton branches, A is the area of a sample, and

$$\rho_{\zeta_1,\zeta_2}(\boldsymbol{k}, \boldsymbol{k}', t) = \langle c_{k\zeta_1}^\dagger c_{k'\zeta_2} \rangle = \mathrm{Tr}(\rho c_{k\zeta_1}^\dagger c_{k'\zeta_2}). \tag{14}$$

Note that $\rho_{-,-}(\boldsymbol{r}, \boldsymbol{r}, t)$ and $\rho_{+,+}(\boldsymbol{r}, \boldsymbol{r}, t)$ correspond to the densities of lower and upper polaritons in the real space, while $\rho_{-,-}(\boldsymbol{k}, \boldsymbol{k}, t)$ and $\rho_{+,+}(\boldsymbol{k}, \boldsymbol{k}, t)$ to corresponding occupancies

in the k space. The terms $\rho_{+,-}(\boldsymbol{k}, \boldsymbol{k}, t)$ and $\rho_{-,+}(\boldsymbol{k}, \boldsymbol{k}, t)$ describe the interbranch correlations.

The dynamic equation (11) for the correlators defined in Eq. (14) reads

$$\partial_t \rho_{\zeta_1,\zeta_2}(\boldsymbol{k}, \boldsymbol{k}', t) = \frac{i}{\hbar}[E_{\zeta_1}(\boldsymbol{k}) - E_{\zeta_2}(\boldsymbol{k}')]\rho_{\zeta_1,\zeta_2}(\boldsymbol{k}, \boldsymbol{k}', t) - \frac{1}{\hbar^2}S. \tag{15}$$

Without the last term on the right-hand side this equation describes coherent (ballistic) polariton propagation. The diffusion of the polaritons occurs due to the scattering on the impurities and this effect is accounted for by the second term in Eq. (15). The detailed derivation of (15) and the expression for the scattering term S can be found in Appendix B. It is worth noticing that the first part of Eq. (15) without scattering term S is an analog of the Schrödinger equation and, therefore, Eq. (15) can be applied not only for description of transport effects but also for description of quantum effects.

Let us make a remark on the applicability of the perturbation theory. The particle transport can be described within the Born-Markov approximation provided that $\frac{\langle E \rangle \tau_0}{\hbar} \gg 1$ [26,30] where $\langle E \rangle$ denotes average particle energy and τ_0 is the relaxation time defined in (30). A similar approach based on the derivation of the equations for a 2×2 density matrix was implemented in [25,26] for the problem of the polariton's spin dynamics.

III. EXCITON TRANSPORT

Before we analyze in detail the case of polaritons, where the role of photonic fraction is essential, let us consider the simpler case of bare excitons. We set the Rabi frequency to zero, $\Omega_R = 0$, and thus reduce the problem to the evolution of a single scalar bosonic field.

The dynamic equations (15) then reduce to

$$\frac{\partial}{\partial t} \rho(\boldsymbol{k}, \boldsymbol{k}', t) = \frac{i}{\hbar}[E(\boldsymbol{k}) - E(\boldsymbol{k}')]\rho(\boldsymbol{k}, \boldsymbol{k}', t) - \frac{1}{\hbar^2}S, \tag{16}$$

where

$$S = \pi \frac{n}{A} \hbar \sum_q |U_q|^2 \{[\rho(\boldsymbol{k}, \boldsymbol{k}', t) - \rho(\boldsymbol{k} + \boldsymbol{q}, \boldsymbol{k}' + \boldsymbol{q}, t)] \\ \times [\delta(E(\boldsymbol{k}) - E(\boldsymbol{k} + \boldsymbol{q})) + \delta(E(\boldsymbol{k}') - E(\boldsymbol{k}' + \boldsymbol{q}))]\}. \tag{17}$$

In these formulas n is the impurity concentration that appears in the scattering term after averaging with respect to random impurity positions, $U_q = \int d^2 r e^{-iqr} V(r)$ is a single impurity potential's Fourier component, and $V(r)$ is a single impurity's potential. The quantity A is the sample area defining the allowed values of q. Taking the limit $A \to \infty$ the summation over q can be substituted with integration $\sum_q \to \frac{A}{(2\pi)^2} \int d^2 q$. So the area A cancels out from the expression for the scattering rate which becomes proportional to $n|U_q|^2$.

Equation (16) with the scattering term (17) well describes two transport regimes in the limits of weak and strong disorder. The first one corresponds to the ballistic transport. Indeed, for a spatially uniform system $U_q = 0$ and then Eq. (16) is nothing else but a well known Schrödinger equation written for the density matrix of a pure state in k representation. In this

regime one recovers a standard dispersion of a wave packet corresponding to a massive quantum particle. The size of an envelope $\Delta r(t)$ given by average radius for axially symmetric distributions with $k_0 = 0$ scales linearly with time [28],

$$\Delta r(t) \xrightarrow{t \to \infty} at. \qquad (18)$$

In the second limit of strong disordered potential, dephasing which accompanies the impurity scattering leads to the fast suppression of the correlations between states corresponding to different k, so that nonzero elements of the matrix of the correlators $\rho(k, k')$ group around its diagonal (see Fig. 5 in Appendix C). The transport is now described by kinetic equations of the Boltzmann type, which can be derived from Eq. (16) by moving to the Wigner representation [31]. The transport of excitons is purely diffusive [27] with asymptotic for the beam width scaling as

$$\Delta r(t) \xrightarrow{t \to \infty} at^{0.5}. \qquad (19)$$

To check that the asymptotics above are correct and to consider the intermediate case of a mixed transport, we performed the numerical simulations of two-dimensional excitonic propagation for different disorder strengths characterized by the parameter $n|U|^2$. We took excitonic mass to be twice the mass of a free electron and used the s-wave approximation for the disorder scattering, taking the corresponding matrix element to be q-independent, $U_{\mathbf{q}} = U$. The initial distribution of excitons was taken in the form of a coherent Gaussian packet

$$\rho(t = 0) \sim e^{-\frac{k_r^2 + k_r'^2}{2\delta k_r}}, \qquad (20)$$

with $\delta k_r = 0.085 \ \mu m^{-1}$. For details about the numerical procedure see Appendix C.

The results are shown in Fig. 2. Panel (a) illustrates the time evolution of an initially coherent wave packet as a function of the disorder strength $\sqrt{n}V$. One sees that the increase of disorder slows down the propagation as expected.

An important parameter characterizing the propagation regime is the propagation exponent, calculated as

$$s(t) = \frac{d \ln(\langle r \rangle)}{d \ln(t)}. \qquad (21)$$

For the ballistic propagation $s = 1$ [see Eq. (18)], while for the diffusive $s = 1/2$ [see Eq. (19)]. The dynamics of the propagation exponent is illustrated by panel (b). One can clearly see that the increase of disorder leads to the gradual decrease of the asymptotic value of s which corresponds to the crossover between ballistic and diffusive regimes.

IV. LOWER POLARITON TRANSPORT

Let us now introduce the coupling between the excitonic and photonic modes, setting $\Omega_R \neq 0$. As was mentioned, in this case the upper and lower polariton branches $E_\pm(k)$ separated in energy by $\hbar\Omega_R$ appear (see Fig. 1). Naturally, the transport on both of these branches strongly depends on the corresponding photonic fraction and is thus defined by corresponding Hopfield coefficients.
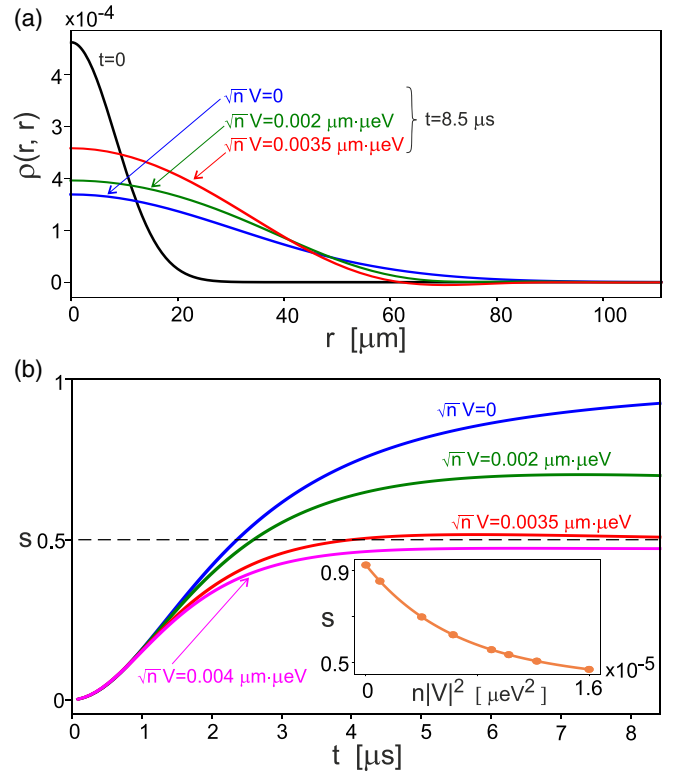

FIG. 2. (a) Time evolution of an initially coherent excitonic wave packet. Black solid line corresponds to the initial density distribution divided by factor 5 to make the scale of the curve comparable to typical scale of the other dependencies; color lines correspond to the density profiles after $t = 8.5 \ \mu s$ for different disordered potential magnitudes $\sqrt{n}U$. (b) The propagation exponent $s(t)$ defined by Eq. (21) as function of time calculated for different disordered potential magnitudes $\sqrt{n}U$. The asymptotic value of this parameter close to 1 characteristic for weak disorder indicates that the transport is ballistic. On the contrary, the asymptotic value close to $1/2$ characteristic for strong disorder is the signature of the purely diffusive propagation. Intermediate values correspond to mixed transport regime. The inset shows the dependence of the asymptotic value of the propagation exponent as function of the disorder strength. The quadratic dispersion of excitons was considered with the effective mass $m_x = 2m_e$.

Let us notice that Eq. (15) contains both intraband correlators $\rho^{++}(k, k')$, $\rho^{--}(k, k')$ defining the distributions of upper and lower polaritons in real space, and cross-band correlators $\rho^{\pm,\mp}(k, k')$. We state the problem as an initial value problem with both intraband correlators corresponding to the upper polariton branch and cross-band correlators equal to zero at $t = 0$. This allows us to eliminate cross-band correlations adiabatically [29] in the limit of $\Omega_R\tau_0 \gg 1$, where

$$\frac{1}{\tau_0} = \frac{2\pi}{\hbar} \frac{n}{A} |U|^2 \sum_{k'} \delta(E_-(k') - E_-(k)). \qquad (22)$$

Indeed, putting

$$\frac{\partial}{\partial t} \rho^{+-} = 0, \qquad (23)$$

we get

$$\rho^{+-} \sim \frac{S(\rho^{+-}, \rho^{++}, \rho^{--})}{E_+(\boldsymbol{k}) - E_-(\boldsymbol{k}')} \sim \rho^{--} \frac{|U^2|}{\Omega_R}. \quad (24)$$

Due to the fact that $E_+(\boldsymbol{k}) - E_-(\boldsymbol{k}') \sim \hbar\Omega_R$ and the scattering terms are bounded from above by τ_0^{-1}, we can estimate

$$\rho^{+-} \sim \frac{\rho^{--}}{\tau_0 \Omega_R}, \quad (25)$$

which vanishes in the limit if $\Omega_R \tau_0 \gg 1$, which is usually satisfied in realistic systems with moderate values of the disorder. Also note that if we assume the scattering to be purely elastic, for moderate disorders the interband scattering becomes impossible because the energy ranges of the upper and the lower polaritons do not overlap.

Under these assumptions and in the s-scattering limit the expression for the scattering term S in Eq. (15) reads for upper and lower polaritons

$$S^{\pm} = \pi \frac{n}{A} \hbar |U|^2 \rho^{\pm}(\boldsymbol{k}, \boldsymbol{k}', t) \sum_{\boldsymbol{q}} [\alpha_{\pm}^2(\boldsymbol{k}) \alpha_{\pm}^2(\boldsymbol{k} + \boldsymbol{q}) \delta(E(\boldsymbol{k}) - E(\boldsymbol{k} + \boldsymbol{q})) + \alpha_{\pm}^2(\boldsymbol{k}') \alpha_{\pm}^2(\boldsymbol{k}' + \boldsymbol{q}) \delta(E(\boldsymbol{k}') - E(\boldsymbol{k}' + \boldsymbol{q}))]$$

$$- \pi \frac{n}{A} \hbar |U|^2 \sum_{\boldsymbol{q}} \rho^{\pm}(\boldsymbol{k} + \boldsymbol{q}, \boldsymbol{k}' + \boldsymbol{q}, t) \alpha_{\pm}(\boldsymbol{k}) \alpha_{\pm}(\boldsymbol{k} + \boldsymbol{q}) \alpha_{\pm}(\boldsymbol{k}') \alpha_{\pm}(\boldsymbol{k}' + \boldsymbol{q}) [\delta(E(\boldsymbol{k}) - E(\boldsymbol{k} + \boldsymbol{q})) + \delta(E(\boldsymbol{k}') - E(\boldsymbol{k}' + \boldsymbol{q}))]. \quad (26)$$

The problem is thus reduced to the problem of the transport of scalar bosons with nonparabolic dispersion. In this work the focus is on lower polaritons, but the case of upper polaritons is fully analogous. As expected, the scattering integral contain the values of the Hopfield coefficients $\alpha_{\pm}(\boldsymbol{k})$, defined by the detuning between the excitonic and photonic modes δ (see Fig. 1). It worth noticing that Eq. (15) with scattering terms (B7) could be used for studying the transport in both strong and weak coupling regimes. However the cases of weak and intermediate coupling are beyond the scope of this paper.

We performed the numerical simulations of the dynamics of lower polaritons for the same initial conditions as in the previous section, creating initially a coherent excitonic Gaussian wave packet given by Eq. (20). We focused on the dependence of the transport regime on detuning δ, varying it in the interval $[-50, -5]$ meV, and set the other parameters as in the paper [20] ($m_{ph} = 0.8 \times 10^{-5} m_e$, $\hbar\Omega_R = 12.5$ meV).

The results are shown in Fig. 3. Panel (a) illustrates the time evolution of an initially coherent lower polariton wave packet as function of the detuning δ for the fixed value of the strength $\sqrt{n}U = 1.5$ μm meV. As one can see, the increase of the negative detuning leading to the increase of the photonic fraction in a lower polariton enhances the propagation. This is expected, as disorder scattering is relevant for the excitonic fraction only.

The dynamics of the propagation exponent for lower polaritons is illustrated by the panel (b). One can clearly see that the increase of negative detuning δ increases the asymptotic value of s and thus corresponds to the crossover between diffusive and ballistic regimes, as was recently reported experimentally [14,20].

We can also derive semiclassical kinetic equations for the upper and lower polaritons, introducing the semi-quasi-classical probability distributions with the help of Wigner representation [31] which could be applied under condition $\frac{\langle E \rangle \tau_0}{\hbar} \gg 1$ at timescales comparable to the relaxation time,

$$\rho_{\pm}(\boldsymbol{k}, \boldsymbol{r}, t) = \int d^2\kappa \rho_{\pm}\left(\boldsymbol{k} + \frac{\kappa}{2}, \boldsymbol{k} - \frac{\kappa}{2}, t\right) \exp(i\kappa\boldsymbol{r}). \quad (27)$$

Assuming the scattering to be elastic so that transitions between the upper and the lower bands are forbidden, and adiabatically eliminating cross-band correlations, one gets from Eqs. (15) and (B7)

$$\frac{\partial}{\partial_t} \rho_{\pm}(\boldsymbol{k}, \boldsymbol{r}, t) + \boldsymbol{v}_{\pm}(\boldsymbol{k}) \cdot \nabla \rho_{\pm}(\boldsymbol{k}, \boldsymbol{r}, t) = S^{\pm}(\rho_{\pm}(\boldsymbol{k}, \boldsymbol{r}, t)), \quad (28)$$

where the scattering integrals are

$$S^{\pm} = -\sum_{\boldsymbol{q}} \frac{2\pi}{\hbar} \frac{n}{A} \alpha_{\pm}^2(\boldsymbol{k} + \boldsymbol{q}) \alpha_{\pm}^2(\boldsymbol{k}) |U_q|^2 \delta(E_{\pm}(\boldsymbol{k} + \boldsymbol{q})$$
$$- E_{\pm}(\boldsymbol{k})) [\rho_{\pm}(\boldsymbol{k}, \boldsymbol{r}, t) - \rho_{\pm}(\boldsymbol{k} + \boldsymbol{q}, \boldsymbol{r}, t)]. \quad (29)$$

These kinetic equations are very similar to the kinetic equations for excitons. The main difference is the presence of Hopfield coefficients in the scattering amplitudes and the difference of the effective masses of the particles (excitons and polaritons) by several orders of magnitude. Let us remark that kinetic equation (28) describes both ballistic and diffusive transport regimes; however, it does not account for quantum effects such as interference.

In the considered limit one can introduce the relaxation times [30] for excitons and polaritons as

$$\frac{1}{\tau_0(\boldsymbol{k})} = \sum_{\boldsymbol{k}'} W_{\boldsymbol{k}'\boldsymbol{k}}, \quad (30)$$

where scattering rates for the excitons and polaritons are given by

$$W_{\boldsymbol{k}'\boldsymbol{k}}^x = \frac{2\pi}{\hbar} \frac{n}{A} |U|^2 \delta(\varepsilon_x(\boldsymbol{k}') - \varepsilon_x(\boldsymbol{k})), \quad (31)$$

$$W_{\boldsymbol{k}'\boldsymbol{k}}^p = \frac{2\pi}{\hbar} \frac{n}{A} |U|^2 \alpha^2(\boldsymbol{k}') \alpha^2(\boldsymbol{k}) \delta(E_p(\boldsymbol{k}') - E_p(\boldsymbol{k})). \quad (32)$$

It can be easily seen that the ratio of the excitonic and polaritonic relaxation times is

$$\frac{\tau_x(\boldsymbol{k})}{\tau_p^{\pm}(\boldsymbol{k})} = \alpha_{\pm}^4(\boldsymbol{k}) \frac{D_p(\boldsymbol{k})}{D_x(\boldsymbol{k})} = \alpha_{\pm}^4(\boldsymbol{k}) \frac{m_p(\boldsymbol{k})}{m_x(\boldsymbol{k})}, \quad (33)$$

where $D_x(\boldsymbol{k})$, $D_p(\boldsymbol{k})$ are the excitonic and polaritonic densities of states.

The dependencies of the relaxation times of lower and upper polaritons on detuning δ are shown in Fig. 4. As expected,
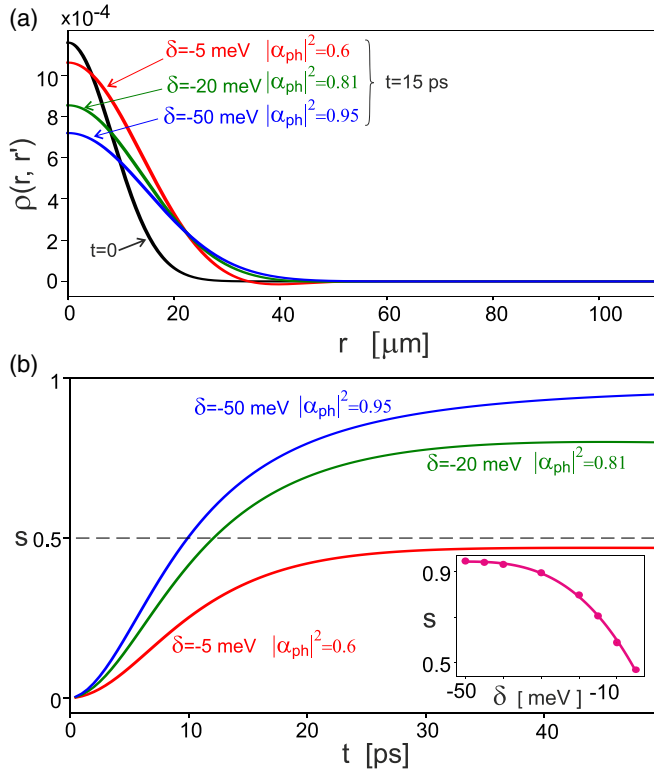
FIG. 3. (a) Time evolution of an initially coherent polaritonic wave packet. The black solid line corresponds to the initial density distribution divided by factor 2 to make the scale of the curve comparable to the characteristic scales of the other curves; the blue, green, and red lines correspond to the density profiles after $t = 15$ ps for different values of the detuning δ. The magnitude of the disorder potential is set to $\sqrt{n}U = 1.5$ μm meV. (b) The propagation exponent $s(t)$ defined by Eq. (21) as function of time calculated for different detunings δ. The asymptotic value of this parameter close to 1 characteristic for big negative detunings and photonic character of lower polaritons indicates that the transport is ballistic. On the contrary, the asymptotic value close to 1/2 characteristic for small negative detunings and the presence of a substantial excitonic fraction in lower polaritons corresponds to the diffusive propagation. Intermediate values correspond to mixed transport regime. The inset shows the dependence of the asymptotic value of the propagation exponent as a function of the detuning and is characteristic of the crossover from the ballistic to diffusive propagation in good agreement with recent experiments [14,20].

polaritonic relaxation times exceed the excitonic relaxation times by several orders of magnitude for realistic experimental conditions. Naturally, the increase of photonic fraction leads to the decrease of the relaxation time. Also we would like to note that the kinetic equations (28) could be used to study weak localization of polaritons [33,34].

V. CONCLUSION

In conclusion, we considered the dynamics of polaritons in a planar microcavity with short-range excitonic disorder. Based on the master equation for the full density matrix of the system and treating the disorder scattering in the Born-Markov approximation we analyzed the crossover between
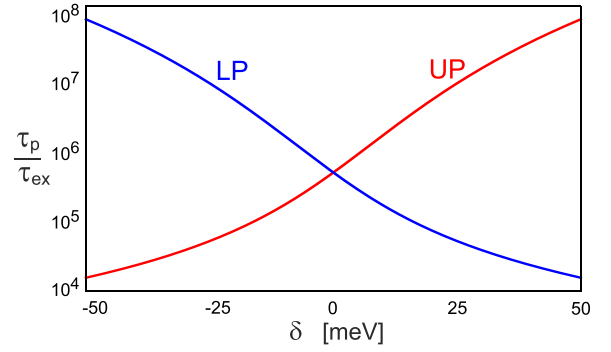

FIG. 4. The ratios of polaritonic and excitonic relaxation times as function of the detuning δ. The blue line corresponds to the lower and the red line to the upper polariton branches. It is seen that the ratio varies by four order of magnitude if the detuning ΔE changes from -50 meV to 50 meV. Such variation of the relaxation times is caused by the change of the effective mass and Hopfield coefficients for upper and lower polaritons.

ballistic and diffusive regimes of the polariton transport with change of the strength of the scattering potential and the detuning between excitonic and photonic modes. We also demonstrated that semiclassical kinetic equations and relaxation times can be obtained for polaritons. Our results are in good agreement with experimental data reported in Refs. [14,20].

APPENDIX A: TAKING THE AVERAGE ON RANDOM IMPURITIES' POSITIONS

We consider uncorrelated delta-functional impurities

$$V_{kk'} = \frac{U_{kk'}}{A} \sum_i \{\exp[-i(k - k')R_i]\}, \quad (A1)$$

where $U_{kk'} = \int d^2r e^{ik-k'r} V(r)$ is the potential Fourier component, and A is the sample area. Factor $1/A$ in the above expression appears due to the plane wave normalization $\psi_k = \frac{e^{ikr}}{\sqrt{A}}$ in the expression for matrix component $V_{kk'} = \langle \psi_k | \hat{V} | \psi_{k'} \rangle$. For this dependency of $V_{kk'}$ on k, k' the averaging can be done analytically representing the averaged term as

$$\left\langle \sum V_{k''k'''} V_{kk'} [c_{k''}^\dagger c_{k'''}, [c_k^\dagger c_{k'}, \rho]] \right\rangle_c$$

$$= \sum \left\langle \sum_{i,j} \exp[-i(k - k')R_i] \exp[-i(k'' - k''')R_j] \right\rangle_c$$

$$\times \frac{U_{k''k'''} U_{kk'}}{A^2} [c_{k''}^\dagger c_{k'''}, [c_k^\dagger c_{k'}, \rho]]. \quad (A2)$$

In the latter expression the inner sum can be calculated

$$\left\langle \sum_{i,j} \exp[-i(\boldsymbol{k}-\boldsymbol{k}')\boldsymbol{R}_i] \exp[-i(\boldsymbol{k}''-\boldsymbol{k}''')\boldsymbol{R}_j] \right\rangle_c$$

$$= N_i \delta_{\boldsymbol{k}-\boldsymbol{k}'+\boldsymbol{k}''-\boldsymbol{k}''',0} = N_i \delta_{\boldsymbol{q}_1+\boldsymbol{q}_2,0}, \quad \text{(A3)}$$

where N_i is the impurity's quantity. Then, finally, we obtain the expression for the averaged term

$$\left\langle \sum V_{\boldsymbol{k}''\boldsymbol{k}'''} V_{\boldsymbol{k}\boldsymbol{k}'} [c^\dagger_{\boldsymbol{k}''} c_{\boldsymbol{k}'''}, [c^\dagger_{\boldsymbol{k}} c_{\boldsymbol{k}'}, \rho]] \right\rangle_c$$

$$= \frac{n}{A} \sum_{\boldsymbol{k},\boldsymbol{k}',\boldsymbol{q}} U_{\boldsymbol{k}',\boldsymbol{k}'-\boldsymbol{q}} U_{\boldsymbol{k},\boldsymbol{k}+\boldsymbol{q}} [c^\dagger_{\boldsymbol{k}'} c_{\boldsymbol{k}'-\boldsymbol{q}}, [c^\dagger_{\boldsymbol{k}} c_{\boldsymbol{k}+\boldsymbol{q}}, \rho]], \quad \text{(A4)}$$

where $n = \frac{N_i}{A}$ is the impurity concentration.

APPENDIX B: DETAILED DERIVATION OF MASTER EQUATION FOR THE POLARITONS

First the expression for $H^I_V(t)$ has to be derived. To do this we can express the $H^I_V(t)$ using the exponent of adjoint representation of H_0,

$$H^I_V(t) = \exp\left(\frac{i}{\hbar}H_0 t\right) H_V \exp\left(-\frac{i}{\hbar}H_0 t\right)$$

$$= \exp\left(\frac{i}{\hbar}t \cdot \boldsymbol{ad}_{H_0}\right) H_V; \quad \text{(B1)}$$

then we calculate the corresponding correlators,

$$[H_0, c^\dagger_{\boldsymbol{k}\sigma_1} c_{\boldsymbol{k}'\sigma_2}] = [E_{\sigma_1}(\boldsymbol{k}) - E_{\sigma_2}(\boldsymbol{k}')] c^\dagger_{\boldsymbol{k}\sigma_1} c_{\boldsymbol{k}'\sigma_2}. \quad \text{(B2)}$$

From this expression it is obvious that we will have a Taylor series for the $e^{E_{\sigma_1}(k)-E_{\sigma_2}(k')}$. Finally using formula (A4) we can calculate the integral and obtain the expression for the scattering part of the master equation (11)

$$\left\langle M_0 \left[H^I_V(t), \int_0^t dt' [H^I_V(t'), \rho^I(t)] \right] M_0^\dagger \right\rangle_c = \frac{n}{A} \sum_{\boldsymbol{k},\boldsymbol{k}',\boldsymbol{q}} U_{\boldsymbol{k}',\boldsymbol{k}'-\boldsymbol{q}} U_{\boldsymbol{k},\boldsymbol{k}+\boldsymbol{q}} \sum_{\sigma_1,\sigma_2,s1,s2=\pm 1} \sigma_1 \cdot \sigma_2 \cdot s_1 \cdot s_2 \alpha_{s_1}(\boldsymbol{k}')$$

$$\times \alpha_{s_2}(\boldsymbol{k}'-\boldsymbol{q}) \alpha_{\sigma_1}(\boldsymbol{k}) \alpha_{\sigma_2}(\boldsymbol{k}+\boldsymbol{q}) f^{\sigma_1,\sigma_2}_{\boldsymbol{k},\boldsymbol{k}+\boldsymbol{q}}(t) [c^\dagger_{\boldsymbol{k}'s_1} c_{\boldsymbol{k}'-\boldsymbol{q}s_2}, [c^\dagger_{\boldsymbol{k}\sigma_1} c_{\boldsymbol{k}+\boldsymbol{q}\sigma_2}, \rho]], \quad \text{(B3)}$$

where $f(t)$ is given by (B8).

The dynamics of the polaritonic pulses in the system can be studied by writing evolution equations for correlators $\rho_{\zeta_1,\zeta_2}(k,k',t) = \langle c^\dagger_{k\pm} c_{k'\pm} \rangle = \mathrm{Tr}(\rho c^\dagger_{k\zeta_1} c_{k'\zeta_2})$. To do this we use the following fact,

$$\mathrm{Tr}\left([c^\dagger_{\boldsymbol{k}'s_1} c_{\boldsymbol{k}'-\boldsymbol{q}s_2}, [c^\dagger_{\boldsymbol{k}\sigma_1} c_{\boldsymbol{k}+\boldsymbol{q}\sigma_2}, \rho]] F \right) = \mathrm{Tr}\left(\rho [c^\dagger_{\boldsymbol{k}\sigma_1} c_{\boldsymbol{k}+\boldsymbol{q}\sigma_2}, [c^\dagger_{\boldsymbol{k}'s_1} c_{\boldsymbol{k}'-\boldsymbol{q}s_2}, F]] \right), \quad \text{(B4)}$$

where F is an arbitrary operator. To prove this expression we need to use several times cycle permutations under the trace operation

$$\mathrm{Tr}([c^\dagger_{\boldsymbol{k}'s_1} c_{\boldsymbol{k}'-\boldsymbol{q}s_2}, [c^\dagger_{\boldsymbol{k}\sigma_1} c_{\boldsymbol{k}+\boldsymbol{q}\sigma_2}, \rho]] F) = \mathrm{Tr}([c^\dagger_{\boldsymbol{k}'s_1} c_{\boldsymbol{k}'-\boldsymbol{q}s_2}, c^\dagger_{\boldsymbol{k}\sigma_1} c_{\boldsymbol{k}+\boldsymbol{q}\sigma_2}\rho - \rho c^\dagger_{\boldsymbol{k}\sigma_1} c_{\boldsymbol{k}+\boldsymbol{q}\sigma_2}] F)$$

$$= \mathrm{Tr}\left[\left(c^\dagger_{\boldsymbol{k}'s_1} c_{\boldsymbol{k}'-\boldsymbol{q}s_2} c^\dagger_{\boldsymbol{k}\sigma_1} c_{\boldsymbol{k}+\boldsymbol{q}\sigma_2}\rho + \rho c^\dagger_{\boldsymbol{k}\sigma_1} c_{\boldsymbol{k}+\boldsymbol{q}\sigma_2} c^\dagger_{\boldsymbol{k}'s_1} c_{\boldsymbol{k}'-\boldsymbol{q}s_2} \right. \right.$$

$$\left. - c^\dagger_{\boldsymbol{k}'s_1} c_{\boldsymbol{k}'-\boldsymbol{q}s_2} \rho c^\dagger_{\boldsymbol{k}\sigma_1} c_{\boldsymbol{k}+\boldsymbol{q}\sigma_2} - c^\dagger_{\boldsymbol{k}\sigma_1} c_{\boldsymbol{k}+\boldsymbol{q}\sigma_2} \rho c^\dagger_{\boldsymbol{k}'s_1} c_{\boldsymbol{k}'-\boldsymbol{q}s_2} \right) F \right]$$

$$= \mathrm{Tr}\left[\rho \left(F c^\dagger_{\boldsymbol{k}'s_1} c_{\boldsymbol{k}'-\boldsymbol{q}s_2} c^\dagger_{\boldsymbol{k}\sigma_1} c_{\boldsymbol{k}+\boldsymbol{q}\sigma_2} + c^\dagger_{\boldsymbol{k}\sigma_1} c_{\boldsymbol{k}+\boldsymbol{q}\sigma_2} c^\dagger_{\boldsymbol{k}'s_1} c_{\boldsymbol{k}'-\boldsymbol{q}s_2} F - c^\dagger_{\boldsymbol{k}\sigma_1} c_{\boldsymbol{k}+\boldsymbol{q}\sigma_2} F c^\dagger_{\boldsymbol{k}'s_1} c_{\boldsymbol{k}'-\boldsymbol{q}s_2} \right. \right.$$

$$\left. \left. - c^\dagger_{\boldsymbol{k}'s_1} c_{\boldsymbol{k}'-\boldsymbol{q}s_2} F c^\dagger_{\boldsymbol{k}\sigma_1} c_{\boldsymbol{k}+\boldsymbol{q}\sigma_2} \right) \right]$$

$$= \mathrm{Tr}\left(\rho [c^\dagger_{\boldsymbol{k}\sigma_1} c_{\boldsymbol{k}\sigma_2}, [c^\dagger_{\boldsymbol{k}'s_1} c_{\boldsymbol{k}'-\boldsymbol{q}s_2}, F]] \right). \quad \text{(B5)}$$

Finally, substituting the $c^\dagger_{\boldsymbol{p}\zeta_1} c_{\boldsymbol{p}'\zeta_2}$ operator instead F and taking into account correlation relations we get the following expression for correlators (B7) which contains four terms corresponding to S_{1-4}:

$$[c^\dagger_{\boldsymbol{k}\sigma_1} c_{\boldsymbol{k}+\boldsymbol{q}\sigma_2}, [c^\dagger_{\boldsymbol{k}'s_1} c_{\boldsymbol{k}'-\boldsymbol{q}s_2}, c^\dagger_{\boldsymbol{p}\zeta_1} c_{\boldsymbol{p}'\zeta_2}]] = [c^\dagger_{\boldsymbol{k}\sigma_1} c_{\boldsymbol{k}+\boldsymbol{q}\sigma_2}, (c^\dagger_{\boldsymbol{k}'s_1}[c_{\boldsymbol{k}'-\boldsymbol{q}s_2}, c^\dagger_{\boldsymbol{p}\zeta_1}]c_{\boldsymbol{p}'\zeta_2} + c^\dagger_{\boldsymbol{p}\zeta_1}[c^\dagger_{\boldsymbol{k}'s_1}, c_{\boldsymbol{p}'\zeta_2}]c_{\boldsymbol{k}'-\boldsymbol{q}s_2})]$$

$$= [c^\dagger_{\boldsymbol{k}\sigma_1} c_{\boldsymbol{k}+\boldsymbol{q}\sigma_2}, (c^\dagger_{\boldsymbol{k}'s_1} c_{\boldsymbol{p}'\zeta_2} \delta_{s_2,\zeta_1} \delta_{\boldsymbol{p}-(\boldsymbol{k}'-\boldsymbol{q}),0} - c^\dagger_{\boldsymbol{p}\zeta_1} c_{\boldsymbol{k}'-\boldsymbol{q}s_2} \delta_{s_1,\zeta_2} \delta_{\boldsymbol{p}'-\boldsymbol{k}',0})]$$

$$= \delta_{s_2,\zeta_1} \delta_{\boldsymbol{p}-(\boldsymbol{k}'-\boldsymbol{q}),0} (c^\dagger_{\boldsymbol{k}\sigma_1}[c_{\boldsymbol{k}+\boldsymbol{q}\sigma_2}, c^\dagger_{\boldsymbol{k}'s_1}]c_{\boldsymbol{p}'\zeta_2} + c^\dagger_{\boldsymbol{k}'s_1}[c^\dagger_{\boldsymbol{k}\sigma_1}, c_{\boldsymbol{p}'\zeta_2}]c_{\boldsymbol{k}+\boldsymbol{q}\sigma_2})$$

$$- \delta_{s_1,\zeta_2} \delta_{\boldsymbol{p}'-\boldsymbol{k}',0} (c^\dagger_{\boldsymbol{k}\sigma_1}[c_{\boldsymbol{k}+\boldsymbol{q}\sigma_2}, c^\dagger_{\boldsymbol{p}\zeta_1}]c_{\boldsymbol{k}'-\boldsymbol{q}s_2} + c^\dagger_{\boldsymbol{p}\zeta_1}[c^\dagger_{\boldsymbol{k}\sigma_1}, c_{\boldsymbol{k}'-\boldsymbol{q}s_2}]c_{\boldsymbol{k}+\boldsymbol{q}\sigma_2})$$

$$= \delta_{s_2,\zeta_1} \delta_{\boldsymbol{p}-(\boldsymbol{k}'-\boldsymbol{q}),0} (c^\dagger_{\boldsymbol{k}\sigma_1} c_{\boldsymbol{p}'\zeta_2} \delta_{s_1,\sigma_2} \delta_{\boldsymbol{k}'-(\boldsymbol{k}+\boldsymbol{q}),0} - c^\dagger_{\boldsymbol{k}'s_1} c_{\boldsymbol{k}+\boldsymbol{q}\sigma_2} \delta_{\zeta_2,\sigma_1} \delta_{\boldsymbol{p}'-\boldsymbol{k},0})$$

$$- \delta_{s_1,\zeta_2} \delta_{\boldsymbol{p}'-\boldsymbol{k}',0} (c^\dagger_{\boldsymbol{k}\sigma_1} c_{\boldsymbol{k}'-\boldsymbol{q}s_2} \delta_{\sigma_2,\zeta_1} \delta_{\boldsymbol{p}-(\boldsymbol{k}+\boldsymbol{q}),0} - c^\dagger_{\boldsymbol{p}\zeta_1} c_{\boldsymbol{k}+\boldsymbol{q}\sigma_2} \delta_{\sigma_1,s_2} \delta_{\boldsymbol{k}-(\boldsymbol{k}'-\boldsymbol{q}),0}). \quad \text{(B6)}$$

Substituting the expression (B7) to Eq. (B4) we obtain the final result (15) with $S = S_1 + S_2 + S_3 + S_4$ where S_{1-4} are given by the following expressions:

$$S_1 = \frac{n}{A} \sum_q U_{k+q,k} U_{k,k+q} \sum_{\sigma_1,\sigma_2=\pm} \sigma_1 \cdot \zeta_1 \alpha_{\sigma_2}(k+q)\alpha_{\zeta_1}(k)\alpha_{\sigma_1}(k)\alpha_{\sigma_2}(k+q) f_{k,k+q}^{\sigma_1,\sigma_2}(t)\rho_{\sigma_1,\zeta_2}(k,k',t), \tag{B7a}$$

$$S_2 = \frac{n}{A} \sum_q U_{k',k'-q} U_{k'-q,k'} \sum_{\sigma_1,\sigma_2=\pm} \sigma_2 \cdot \zeta_2 \alpha_{\zeta_2}(k')\alpha_{\sigma_1}(k'-q)\alpha_{\sigma_1}(k'-q)\alpha_{\sigma_2}(k') f_{k'-q,k'}^{\sigma_1,\sigma_2}(t)\rho_{\zeta_1,\sigma_2}(k,k',t), \tag{B7b}$$

$$S_3 = \frac{n}{A} \sum_q U_{k+q,k} U_{k',k'+q} \sum_{\sigma_1,\sigma_2=\pm} \sigma_1 \cdot \sigma_2 \cdot \zeta_1 \cdot \zeta_2 \alpha_{\sigma_1}(k+q)\alpha_{\zeta_1}(k)\alpha_{\zeta_2}(k')\alpha_{\sigma_2}(k'+q) f_{k',k'+q}^{\zeta_2,\sigma_2}(t)\rho_{\sigma_1,\sigma_2}(k+q,k'+q,t), \tag{B7c}$$

$$S_4 = \frac{n}{A} \sum_q U_{k',k'-q} U_{k-q,k} \sum_{\sigma_1,\sigma_2=\pm} \sigma_1 \cdot \sigma_2 \cdot \zeta_1 \cdot \zeta_2 \alpha_{\zeta_2}(k')\alpha_{\sigma_2}(k'-q)\alpha_{\sigma_1}(k-q)\alpha_{\zeta_1}(k) f_{k-q,k}^{\sigma_1,\zeta_1}(t)\rho_{\sigma_1,\sigma_2}(k-q,k'-q,t). \tag{B7d}$$

The functions

$$f_{k,k'}^{\sigma_1,\sigma_2}(t) = \frac{1 - \exp\left\{-\frac{i}{\hbar}t[E_{\sigma_1}(k) - E_{\sigma_2}(k')]\right\}}{\frac{i}{\hbar}[E_{\sigma_1}(k) - E_{\sigma_2}(k')]}. \tag{B8}$$

The particle transport can be described within the Born-Markov approximation provided that $\frac{\langle E \rangle \tau_0}{\hbar} \gg 1$ where $\langle E \rangle$ denotes the average particle energy; τ_0 is the relaxation time defined in Eq. (30) [30],

$$f_{k,k'}^{\sigma_1,\sigma_2}(t) \xrightarrow{t \gg \Delta_E} \pi \hbar \delta(E_{\sigma_1}(k) - E_{\sigma_2}(k')), \tag{B9}$$

and corresponds therefore to the energy conservation during a scattering act.

APPENDIX C: NUMERICAL PROCEDURE

1. Numerical procedure for only excitonic problem

In the 2D microcavity the elasticity of scattering fixes the length of the wave vector after scattering $|\tilde{k}| = |k|$. Thus we can move from integration with respect to d^2q to integration with respect to $\tilde{k} = k + q$. And then moving to the polar coordinates and considering properties of δ functions, the following formulas for (17) were obtained,

$$S_{2D}(k,k') = \pi n \hbar |U|^2 \rho(k,k',t)[D_{2D}(k) + D_{2D}(k')]$$
$$\qquad - \pi n \hbar |U|^2 (I_k + I_{k'}), \tag{C1}$$

$$I_k = \frac{1}{(2\pi)^2} \int d\theta_{\tilde{k}} \left[k \frac{\rho(\tilde{k}, k' - k + \tilde{k}, t)}{\hbar |v_k|} \right], \tag{C2}$$

$$I_{k'} = \frac{1}{(2\pi)^2} \int d\theta_{\tilde{k}'} \left[k' \frac{\rho(k - k' + \tilde{k}, \tilde{k}', t)}{\hbar |v_{k'}|} \right], \tag{C3}$$

where $D_{2D}(k)$ is a density of states. Equation (16) in this case can be reduced to the system of ODEs with-time independent coefficients by introducing a mesh in k, k' space (see Fig. 5). However, if we take N points for $|k|$ discretization and N_θ for θ discretization we have a total number of $N^2 N_\theta^2$ parameters for density matrix $\rho(k, k')$ and $N^2 N_\theta^3$ complexity of calculation of the ODE's system right part which makes this numerical problem enormous. Fortunately, for the case when the initial reversal space distribution profile has axial symmetry such as a Gaussian profile with $k_0 = 0$ it is possible to reduce the total number of parameters to $N^2 N_\theta$ and the total right

part calculation complexity to $N^2 N_\theta^2$, which is much better. In the axial symmetric case the density matrix has symmetry $\rho(\hat{R}(\theta)k, \hat{R}(\theta)k', t) = \rho(k, k', t)$, so we can for example fix the direction of $k = [|k|, 0]$ and reduce the number of parameters. Finally, the equidistant mesh in $k, k', \theta_{k'}$ were considered. The integrals in (C1) were approximately replaced by sums and interpolation was used to approximate points appearing in the integral approximations which are not contained in the mesh. Now

$$\rho(r, r, t) \sim \int dk dk' d\theta d\theta' kk' e^{-ikr\cos(\theta) + ik'r\cos(\theta' + \theta)}$$
$$\times \rho(k, k', \theta', t)$$
$$= \int dk dk' d\theta' kk' 2\pi J_0(q(k, k', \theta')r)\rho(k, k', \theta', t), \tag{C4}$$

where J_0 is the zero-order Bessel function, and $q = |k - k'| = \sqrt{k'^2 + k^2 - 2kk'\cos(\theta')}$ gives us the real-space distribution. The accurate calculation of this integral with the function oscillating very fast is also an ambitious task. The normalization condition $2\pi \int dx x \rho(x, x, 0) = 1$ was taken.
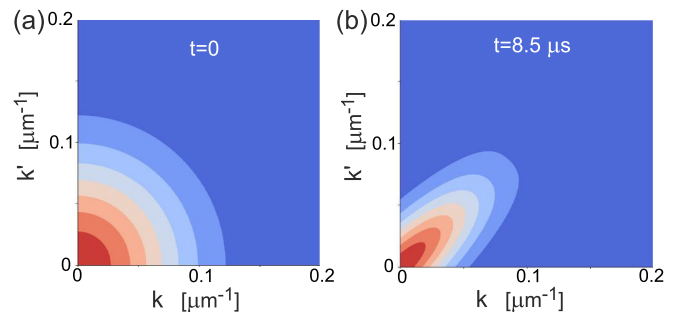

FIG. 5. The pallet shows the initial $\rho(k_r, k'_r, \theta = 0, t = 0)$ and final $\rho(k_r, k'_r, \theta = 0, t = 8.5 \text{ μs})$ k_r-space distribution profiles for the diffusive case $\sqrt{n}U = 0.004$ μeV μm. In the diffusive case the profile constricts to the line $k_r = k'_r$ which corresponds to field becoming more classical. One can recall that the kinetic equation for semiclassical probability distribution $\rho(k, r, t)$ can be derived from the master equation (16) using Wigner representation [31] $\rho(k + \frac{\kappa}{2}, k - \frac{\kappa}{2}, t)$ and making expansion on small κ.

2. Numerical procedure for lower-band polaritons

For the lower-band polaritons the master equation looks as follows:

$$S = \pi\hbar\frac{n}{A}|U|^2 \sum_{\boldsymbol{q}}\{\rho(\boldsymbol{k},\boldsymbol{k}',t)[\alpha^2(k)\alpha^2(\boldsymbol{k}+\boldsymbol{q})\delta(E(\boldsymbol{k})-E(\boldsymbol{k}+\boldsymbol{q})) + \alpha^2(k')\alpha^2(\boldsymbol{k}'+\boldsymbol{q})\delta(E(\boldsymbol{k}')-E(\boldsymbol{k}'+\boldsymbol{q}))]\}$$

$$- \pi\hbar\frac{n}{A}|U|^2 \sum_{\boldsymbol{q}}\rho(\boldsymbol{k}+\boldsymbol{q},\boldsymbol{k}'+\boldsymbol{q},t)\alpha(\boldsymbol{k})\alpha(\boldsymbol{k}+\boldsymbol{q})\alpha(\boldsymbol{k}')\alpha(\boldsymbol{k}'+\boldsymbol{q})[\delta(E(\boldsymbol{k})-E(\boldsymbol{k}+\boldsymbol{q})) + \delta(E(\boldsymbol{k}')-E(\boldsymbol{k}'+\boldsymbol{q}))]. \quad \text{(C5)}$$

The resulting equation is similar to (C1) with inclusion of Hopfield coefficients α. The numerical procedure stays the same.

[1] D. Sanvitto, F. Pulizzi, A. J. Shields, P. C. Christianen, S. N. Holmes, M. Y. Simmons, D. A. Ritchie, J. C. Maan, and M. Pepper, Observation of charge transport by negatively charged excitons, Science **294**, 837 (2001).

[2] B. A. Gregg, Excitonic solar cells, J. Phys. Chem. B **107**, 4688 (2003).

[3] G. Banappanavar, S. Vaidya, U. Bothra, L. R. Hegde, K. P. Sharma, R. H. Friend, and D. Kabra, Novel optoelectronic technique for direct tracking of ultrafast triplet excitons in polymeric semiconductor, Appl. Phys. Rev. **8**, 031415 (2021).

[4] A. Classen, C. L. Chochos, L. Lüer, V. G. Gregoriou, J. Wortmann, A. Osvet, K. Forberich, I. McCulloch, T. Heumüller, and C. J. Brabec, The role of exciton lifetime for charge generation in organic solar cells at negligible energy-level offsets, Nat. Energy **5**, 711 (2020).

[5] A. J. Gillett, A. Privitera, R. Dilmurat, A. Karki, D. Qian, A. Pershin, G. Londi, W. K. Myers, J. Lee, J. Yuan et al., The role of charge recombination to triplet excitons in organic solar cells, Nature (London) **597**, 666 (2021).

[6] G. M. Akselrod, P. B. Deotare, N. J. Thompson, J. Lee, W. A. Tisdale, M. A. Baldo, V. M. Menon, and V. Bulović, Visualization of exciton transport in ordered and disordered molecular solids, Nat. Commun. **5**, 3646 (2014).

[7] O. V. Mikhnenko, P. W. Blom, and T.-Q. Nguyen, Exciton diffusion in organic semiconductors, Energy Environ. Sci. **8**, 1867 (2015).

[8] M. Kulig, J. Zipfel, P. Nagler, S. Blanter, C. Schüller, T. Korn, N. Paradiso, M. M. Glazov, and A. Chernikov, Exciton Diffusion and Halo Effects in Monolayer Semiconductors, Phys. Rev. Lett. **120**, 207401 (2018).

[9] E. Fortin, S. Fafard, and A. Mysyrowicz, Exciton Transport in Cu_2O: Evidence for Excitonic Superfluidity?, Phys. Rev. Lett. **70**, 3951 (1993).

[10] S. Deng, E. Shi, L. Yuan, L. Jin, L. Dou, and L. Huang, Long-range exciton transport and slow annihilation in two-dimensional hybrid perovskites, Nat. Commun. **11**, 664 (2020).

[11] J. Rudolph, R. Hey, and P. V. Santos, Long-Range Exciton Transport by Dynamic Strain Fields in a GaAs Quantum Well, Phys. Rev. Lett. **99**, 047602 (2007).

[12] D. Ballarini, D. Caputo, C. S. Muñoz, M. De Giorgi, L. Dominici, M. H. Szymańska, K. West, L. N. Pfeiffer, G. Gigli, F. P. Laussy, and D. Sanvitto, Macroscopic Two-Dimensional Polariton Condensates, Phys. Rev. Lett. **118**, 215301 (2017).

[13] P. Borri, W. Langbein, U. Woggon, J. R. Jensen, and J. M. Hvam, Microcavity polariton linewidths in the weak-disorder regime, Phys. Rev. B **63**, 035307 (2000).

[14] M. Balasubrahmaniyam, A. Simkhovich, A. Golombek, G. Sandik, G. Ankonina, and T. Schwartz, From enhanced diffusion to ultrafast ballistic motion of hybrid light-matter excitations, Nat. Mater. **22**, 338 (2023).

[15] D. M. Myers, S. Mukherjee, J. Beaumariage, D. W. Snoke, M. Steger, L. N. Pfeiffer, and K. West, Polariton-enhanced exciton transport, Phys. Rev. B **98**, 235302 (2018).

[16] E. Orgiu, J. George, J. Hutchison, E. Devaux, J. Dayen, B. Doudin, F. Stellacci, C. Genet, J. Schachenmayer, C. Genes et al., Conductivity in organic semiconductors hybridized with the vacuum field, Nat. Mater. **14**, 1123 (2015).

[17] G. Lerario, D. Ballarini, A. Fieramosca, A. Cannavale, A. Genco, F. Mangione, S. Gambino, L. Dominici, M. De Giorgi, G. Gigli et al., High-speed flow of interacting organic polaritons, Light Sci. Appl. **6**, e16212 (2017).

[18] S. Hou, M. Khatoniar, K. Ding, Y. Qu, A. Napolov, V. M. Menon, and S. R. Forrest, Ultralong-range energy transport in a disordered organic semiconductor at room temperature via coherent exciton-polariton propagation, Adv. Mater. **32**, 2002127 (2020).

[19] G. G. Rozenman, K. Akulov, A. Golombek, and T. Schwartz, Long-range transport of organic exciton-polaritons revealed by ultrafast microscopy, ACS Photonics **5**, 105 (2018).

[20] M. Wurdack, E. Estrecho, S. Todd, T. Yun, M. Pieczarka, S. Earl, J. Davis, C. Schneider, A. Truscott, and E. Ostrovskaya, Motional narrowing, ballistic transport, and trapping of room-temperature exciton polaritons in an atomically-thin semiconductor, Nat. Commun. **12**, 5366 (2021).

[21] Q. Guo, B. Wu, R. Du, J. Ji, K. Wu, Y. Li, Z. Shi, S. Zhang, and H. Xu, Boosting exciton transport in WSe_2 by engineering its photonic substrate, ACS Photonics **9**, 2817 (2022).

[22] V. Savona, C. Piermarocchi, A. Quattropani, F. Tassone, and P. Schwendimann, Microscopic Theory of Motional Narrowing of Microcavity Polaritons in a Disordered Potential, Phys. Rev. Lett. **78**, 4470 (1997).

[23] I. G. Savenko, E. B. Magnusson, and I. A. Shelykh, Density-matrix approach for an interacting polariton system, Phys. Rev. B **83**, 165316 (2011).

[24] H. J. Carmichael, Statistical Methods in Quantum Optics 1: Master Equations and Fokker-Planck Equations, Theoretical and Mathematical Physics, 1st ed. (Springer, Berlin, Heidelberg, 2013), p. 361.

[25] C. Grimaldi, Electron spin dynamics in impure quantum wells for arbitrary spin-orbit coupling, Phys. Rev. B **72**, 075307 (2005).

[26] N. S. Averkiev and M. M. Glazov, Specific features of optical orientation and relaxation of electron spins in quantum wells with a large spin splitting, Semiconductors **42**, 958 (2008).

[27] M. M. Glazov, Phonon wind and drag of excitons in monolayer semiconductors, Phys. Rev. B **100**, 045426 (2019).

[28] V. M. Agranovich and Y. N. Gartstein, Nature and dynamics of low-energy exciton polaritons in semiconductor microcavities, Phys. Rev. B **75**, 075302 (2007).

[29] E. Brion, L. H. Pedersen, and K. Mølmer, Adiabatic elimination in a lambda system, J. Phys. A: Math. Theor. **40**, 1033 (2007).

[30] E. M. Lifschitz and L. P. Pitajewski, *Physical Kinetics*, Course of Theoretical Physics, Vol. 10 (Butterworth-Heinemann, 1981).

[31] A. Altland and B. D. Simons, *Condensed Matter Field Theory*, 2nd ed. (Cambridge University Press, Cambridge, 2010).

[32] Y. Sun, P. Wen, Y. Yoon, G. Liu, M. Steger, L. N. Pfeiffer, K. West, D. W. Snoke, and K. A. Nelson, Bose-Einstein Condensation of Long-Lifetime Polaritons in Thermal Equilibrium, Phys. Rev. Lett. **118**, 016602 (2017).

[33] M. I. Dyakonov, Magnetoconductance due to weak localization beyond the diffusion approximation: The high-field limit, Solid State Commun. **92**, 711 (1994).

[34] A. P. Dmitriev, V. Y. Kachorovskii, and I. V. Gornyi, Non-backscattering contribution to weak localization, Phys. Rev. B **56**, 9910 (1997).